Quim. Nova, Vol. 39, No. 10, 1151-1158, 2016 http://dx.doi.org/10.21577/0100-4042.20160152

Artigo

A NEW RHODAMINE B DERIVATIVE RBMAB AS A HIGHLY SELECTIVE AND SENSITIVE CHEMOSENSOR FOR Fe^{3+} WITH LOW DETECTION LIMIT

Wei Shen[a,*], Lin Wang[b], Min Chen[a] and Hongfei Lu[b,#]
[a]School of Sciences, Nanjing Agricultural University, 1 Tongwei Road, 210095 Nanjing, China
[b]School of Biology and Chemical Engineering, Jiangsu University of Science and Technology, 2 Mengxi Road, 212003 Zhenjiang, China

Recebido em 11/02/2016; aceito em 22/06/2016; publicado na web em 26/08/2016

A new Rhodamine B derivative RBMAB, namely 3-amino-N-(2-(3',6'-bis (diethylamino)-3-oxospiro[isoindoline-1,9'-xanthen]-2-yl) ethyl)benzamide, was designed, synthesized and structurally characterized to develop a chemosensor. The studies show that RBMAB exhibits high selectivity toward Fe^{3+} among many other metal cations in an ethanol-H_2O (3:2, v/v, PBS buffer, 1.2 mmol L^{-1}, pH 7.2) solution. It has a low detection limit of 0.021μm. Fluorescence microscopy experiments further demonstrate that RBMAB can be used as a fluorescent probe to detect Fe^{3+} in living cells.

Keywords: rhodamine B derivative; chemosensor; Fe^{3+}; cell imaging.

INTRODUCTION

Fe^{3+} is transitional metal ion and it is one of the most important trace elements in biological systems for Fe^{3+} provides the oxygen--carrying capacity of heme, so, iron in small concentrations is essential to human health.[1] But its deficiency or overload can induce serious disorders and infectious diseases such as anemia,[2] hemochromatosis,[3] malaria,[4] Parkinson,[5] Alzheimer.[6] Many techniques for detecting Fe^{3+} have been reported, including atomic absorption spectrometry,[7,8] voltammetry,[9] fluorometric and colorimetric method.[10-13] Many are complicated and not suitable for quick and online monitoring. Among these methods, fluorometric assay with specific fluorescence chemosensor is currently attracting much attention as a method to reveal the molecular functions of the ions in living systems.

Rhodamine B-based fluorescent sensors have attracted considerable interest for their excellent photo-physical properties, high fluorescence quantum yield and visible-wavelength excitation.[14] Rhodamine B moiety also owns "off-on" ability, when specific metal ions bind to rhodamine derivatives, it will start ring open process to cause strong fluorescence emission.[15] Many of rhodamine derivatives have been designed and synthesized to display specific detection of Pb^{2+}, Cu^{2+}, Cd^{2+}, Cr^{3+}, Hg^{2+}.[16-27] Although rhodamine based sensors for Fe^{3+} have been reported a lot. Quite a lot of them haven't present the detection limit or have comparative high detection limit which hindered for low concentration detection.[28-35]

In this paper, we present a new rhodamine B derivative, 3-amino-N-(2-(3',6'-bis (diethylamino)-3-oxospiro[isoindoline-1,9'-xanthen]-2-yl)ethyl)benzamide. It exhibits high sensitivity toward Fe^{3+} among many other metal cations in an ethanol-H_2O (3:2, v/v, PBS buffer, 1.2 mmol L^{-1}, pH 7.2) solution. It has a low detection limit of 0.021 μm. Cell studies further demonstrate that RBMAB can be a potential probe to detect Fe^{3+} in human liver cells (L-02).

EXPERIMENTAL

Materials and instrumentation

All reagents and organic solvents that used were of ACS grade or higher and were used without further purification. Unless otherwise noted, all chemicals were purchased from J&K Scientific Shanghai, China) and used as received. All solvents were of analytical grade, and double-distilled water was used in all experiments. The salts that were used to prepare metal ion stock solutions were $AgNO_3$, $AlCl_3$, $Ba(NO_3)_2$, $CaCl_2$, $CdCl_2{\cdot}2.5H_2O$, $CoCl_2{\cdot}6H_2O$, $CrCl_3{\cdot}6H_2O$, $IrCl_3$, CuCl, $CuCl_2{\cdot}2H_2O$, $FeCl_2{\cdot}4H_2O$, $FeCl_3{\cdot}6H_2O$, $HgCl_2$, KCl, $LiCl{\cdot}H_2O$, $MgCl_2{\cdot}6H_2O$, $MnCl_2{\cdot}4H_2O$, NaCl, $NiCl_2{\cdot}6H_2O$, $PbCl_2$, $SnCl_2{\cdot}H_2O$ and $ZnCl_2$. Thin-layer chromatography was performed on a HAIYANG silica gel F254 plate, and compounds were visualized under UV light (λ = 254 nm). Column chromatography was performed using HAIYANG silica gel (type: 200–300 mesh ZCX-2).

^1H (500 MHz) and ^{13}C NMR (126 MHz) spectra were recorded on an Avance 500 spectrometer (Bruker; Billerica, MA, USA). The chemical shifts are reported in δ units (ppm) downfield relative to the chemical shift of tetramethylsilane. The abbreviations br, s, d, t and m denote broad, singlet, doublet, triplet and multiplet, respectively. Mass spectra were obtained with a Finnigan TSQ Quantum LC/MS Spectrometer. High-resolution mass spectra (HRMS) were acquired under electron ionization conditions with a double-focusing high--resolution instrument (Autospec; Micromass Inc.). The pH levels of stock solutions were measured using a PHS-25C Precision pH/mV Meter (Aolilong, Hangzhou, China). UV–Vis and fluorescence spectra were obtained on a UV-1700 UV–VIS-NIR spectrophotometer (Shimadzu, Japan) and a Fluoroscopy Max-4 (Horiba, Japan), respectively, at room temperature.

Synthesis of 2-(2-aminoethyl)-3', 6'-bis (diethylamino) spiro[isoindoline-1,9'- xanthen]-3-one (1)

Synthesis of compound 1 was according to the reported procedure.[36]

*e-mail: swgdj@njau.edu.cn
#Alternative e-mail: zjluhf1979@hotmail.com

Synthesis of 3-amino-N-(2-(3', 6'-bis (diethylamino)-3-oxospiro [isoindoline-1, 9'-xanthen]-2-yl)ethyl)benzamide (RBMAB)

To a solution of 3-aminobenzoic acid (50 mg, 0.356 mmol) in 5 mL of DMSO were added DCC (113 mg, 0.547 mmol) and HOBt (74 mg, 0.547 mmol),then stirred for 20 minutes before adding compound **1** (265 mg, 0.547 mmol) and triethylamine (0.098 mL, 0.547 mmol). The reacting mixture was refluxed at 80 °C for 12 h. Water was added to the mixture, and then extracted three times with ethyl. The organic layer was dried with anhydrous sodium sulfate and then concentrated. Flash chromatography (silica gel; MeOH/CH_2Cl_2, 1:99; v:v) of the crude mixture afforded RBMAB (158 mg) in 71.8% yield as a brown-yellow solid.^{1}H NMR (500 MHz, $CDCl_3$) δ 8.15 (s, 1H), 7.95 (dd, J = 5.8, 2.7 Hz, 1H), 7.48 (dd, J = 5.4, 3.2 Hz, 2H), 7.36-7.15 (m, 6H), 7.11 (dd, J = 5.8, 2.6 Hz, 1H), 6.81 (d, J = 7.2 Hz, 1H), 6.48 (d, J = 8.8 Hz, 4H), 6.31 (d, J = 6.8 Hz, 2H), 3.45 (d, J = 4.8 Hz, 2H), 3.35 (h, J = 8.5 Hz, 8H), 3.18 (s, 2H), 1.19 (t, J = 7.0 Hz, 12H).^{13}C NMR (126 MHz, $CDCl_3$) δ 170.26, 167.18, 153.91, 153.24, 148.83, 146.58, 135.39, 132.82, 130.33, 129.36, 128.41, 128.16, 123.89, 122.87, 117.66, 116.96, 113.99, 108.40, 104.73, 97.90, 77.29, 77.03, 76.78, 65.85, 53.42, 44.43, 41.73, 39.89, 29.68, 12.56. HRMS (M^++1) found, 604.3292; calculated for $C_{34}H_{41}N_4O_5^+$, 604.3288.

General procedure of UV-Vis and fluorescence-spectral studies

Stock solutions (10^{-3} mol L^{-1}) of the chloride or nitrate salts of Ag^+, Al^{3+}, Ba^{2+}, Ca^{2+}, Cd^{2+}, Co^{2+}, Cr^{3+}, Cs^{2+}, Cu^+, Cu^{2+}, Fe^{2+}, Fe^{3+}, Hg^{2+}, K^+, Li^+, Mg^{2+}, Mn^{2+}, Na^+, Ni^{2+}, Pb^{2+} and Zn^{2+}, in deionized water were prepared. The stock solution of RBMAB (10 mol L^{-1}) was prepared in ethanol/PBS (3:2; v/v; 1.2 mmol L^{-1} , pH 7.2). Working solutions of RBMAB were freshly prepared by diluting the highly concentrated stock solution to the desired concentration prior to the spectroscopic measurements.

All experiments were performed in an ethanol/PBS (3:2; v/v; 1.2 mmol L^{-1}, pH 7.2) solution. In each titration experiment, a 20 μmol L^{-1} solution of the probe RBMAB was placed in a quartz optical cell with a 1-cm optical path length, and the appropriate amount of ion stock solution was added to the quartz optical cell using a micropipette. Spectral data were recorded 120 min after the ion addition. In the selectivity experiments, the test samples were prepared by placing an appropriate amount of the cation stock solution in 3 mL of the probe RBMAB solution (20 μmol L^{-1}). In the fluorescence measurements, excitation was provided at 562 nm, and emission was collected from 590 to 700 nm.

Cell studies

In vitro experiments were performed using human L-02 cells. L-02 cells were cultured in RPMI-1640 medium, which was supplemented with 10% fetal bovine serum (FBS) in an atmosphere of 5% CO_2 at 37 °C. The cytotoxicity of RBMAB was determined using an MTT assay. Briefly, the cells were incubated with different concentrations of RBMAB for 48 h. The cell viability was evaluated by incubating with 0.5 mg mL^{-1} 3-[4,5-dimethylthiazol-2-yl]-2,5--diphenyltetrazolium bromide (MTT) for 4 h under 5% CO_2/95% air at 37 °C. The media were replaced with 100uL of DMSO, and the absorbance was read at 570 nm. For fluorescence microscopy images, one day before imaging, the cells were seeded in 6-well plates. Immediately before the experiments, the cells were incubated with 0.1 mmol L^{-1} $FeCl_3$ in 50 mmol L^{-1} PBS buffer for 120 min at room temperature, followed by incubation with 20 μmol L^{-1} RBMAB at 37 °C under 5% CO_2 for additional 30 min. The cells were washed with PBS three times and subsequently imaged. The fluorescence intracellular imaging was observed under an Olympus inverted fluorescence microscope with a 20× objective lens multiplied by 1.6 (excited with green light). The cells that were incubated with the solvent DMSO were taken as a control.

RESULT AND DISCUSSION

Synthesis of RBMAB

The synthesis procedure of RBMAB is illustrated in Scheme 1. Compound **1** was prepared in a 92% yield from commercially available rhodamine B and ethane-1,2- diamine.[36] RBMAB was prepared in a 71.8% yield by the reaction of 3-aminobenzoic acid with 1.5 equiv of compound 1, 1.5 equiv of DCC, 1.5 equiv of HOBt and 1.5 equiv of triethylamine in DMSO for 12 h. The structure of RBMAB was confirmed by ^{1}H NMR, ^{13}C NMR and HRMS (Supporting materials).

Responses of RBMAB to pH

To investigate the pH response of probe RBMAB, acid-base

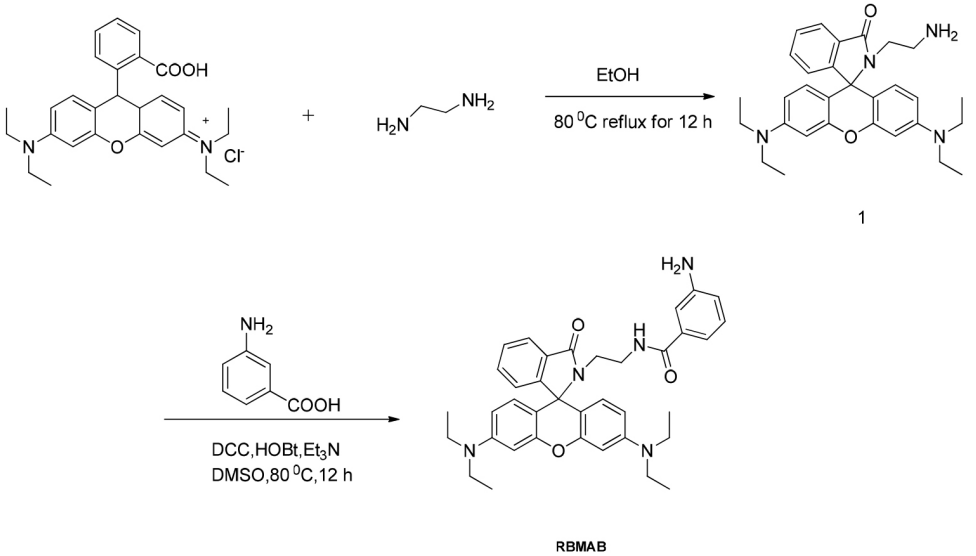

Scheme 1 *Synthesis of RBMAB*

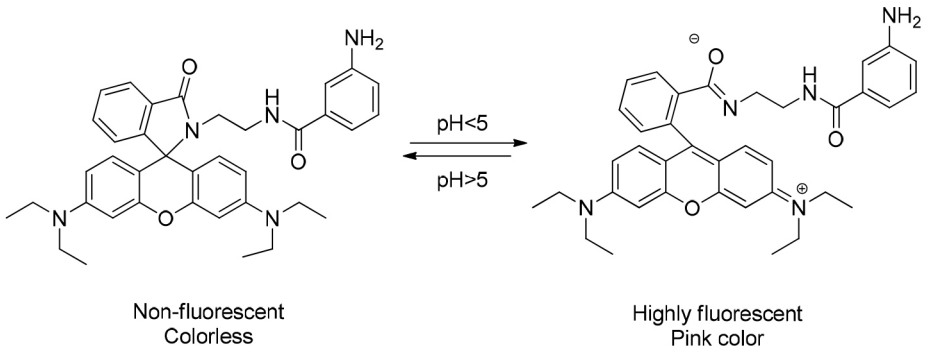

Scheme2 Mechanism *of the response of RBMAB to pH changes*

titration experiments were performed in EtOH/H_2O (3:2, v/v) solutions. The fluorescence intensities of RBMAB at 582 nm at different pH values (1.02, 2.05, 2.94, 4.07, 5.08, 6.02, 7.05, 7.96, 9.03 and 10.06) were recorded. As shown in Figure 1, RBMAB did not emit any distinct and characteristic fluorescence (λ_{ex} = 562 nm) in the pH range of 5.0-10.0, the result indicated that the spirolactam form of RBMAB was the predominant species (Scheme 2). When the pH was adjusted to between 1.0 and 5.0, the fluorescence intensity at 582 nm was apparently enhanced due to the ring-opening process of the spirocyclic moiety of Rhodamine B (Scheme 2).[19,20] These results showed that RBMAB was insensitive to pH from 5.0 to 10.0 and may work under approximately physiological conditions with very low background fluorescence. Therefore, further UV-vis and fluorescence studies were carried out in a EtOH/H_2O (3:2 v/v, PBS buffer, 1.2 mmol L^{-1}, pH 7.2) solution.

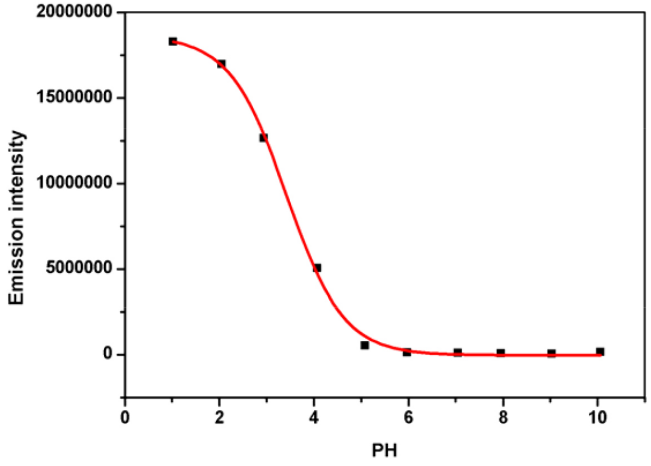

Figure 1. *Effect of pH on the fluorescence of RBMAB (20 μmol L^{-1}) in ethanol-H_2O solutions (3:2 v/v). The excitation and emission wavelengths were 562 nm and 582 nm, respectively*

Response time of RBMAB

The response time of the reaction system was also a very important aspect as a chemical sensor for practical applications. So the response time of the reaction system was also investigated to evaluate the sensitivity of RBMAB toward Fe^{3+}. To an optical quartz cell with a 1-cm path length containing RBMAB (20 μmol L^{-1}) in a EtOH/H_2O (3:2 v/v, PBS buffer, 1.2 mmol L^{-1}, pH 7.2) solution, Fe^{3+} (200 μmol L^{-1}, 10 equiv) was added. The change in the fluorescence intensity of RBMAB over a period of 200 min was recorded. As shown in Figure 2, the fluorescence intensity of RBMAB at 582 nm slowly increased in the first 120 min, and then hold steady, which indicates that the reaction system was stable after 120 min. Therefore, a 120-min reaction time was selected in subsequent experiments to ensure that the metal ions had enough time to sufficiently chelate with the sensor.

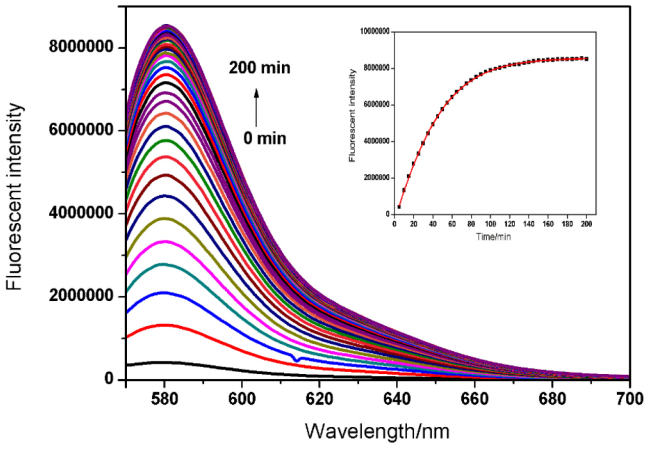

Figure 2. *Fluorescence spectra of RBMAB (20 μmol L^{-1}) with Fe^{3+} (200 μmol L^{-1}, 10 eq.). The excitation and emission wavelengths were 562 and 582 nm, respectively.* ***Inset****: plot of the fluorescence intensities at 582 nm over a period of 180 min.*

UV-vis spectral response of RBMAB

To evaluate the selectivity of RBMAB for Fe^{3+}, the sensing ability of RBMAB toward different metal cations was studied using UV-Vis spectroscopy. As shown in Figure 3, the UV-vis spectrum of RBMAB (20 μmol L^{-1}) in an ethanol-H_2O (3:2 v/v, PBS buffer, 1.2 mmol L^{-1}, pH 7.2) solution exhibits notably weak absorbance at 562 nm. The addition of 10 equiv. Fe^{3+} (200 μmol L^{-1}) into the solution significantly enhances the absorbance at 562 nm. Under the identical condition, no obvious response was observed at 562 nm after other metal ions Al^{3+}, Ba^{2+}, Ca^{2+}, Cd^{2+}, Co^{2+}, Cr^{3+}, Cs^{2+}, Cu^{+}, Cu^{2+}, Fe^{2+}, Fe^{3+}, Hg^{2+}, K^{+}, Li^{+}, Mg^{2+}, Mn^{2+}, Na^{+}, Ni^{2+}, Pb^{2+} and Zn^{2+} were added, while a relative small enhancement by addition of Ag^{+}. The results demonstrate that RBMAB can serve as an excellent selective chemosensor for Fe^{3+} in an ethanol-H_2O (3:2 v/v, PBS buffer, 1.2 mmol L^{-1}, pH 7.2) solution.

To determine the binding stoichiometry of the RBMAB- Fe^{3+} complex, a Job's plot was generated by continuously varying the mole fraction of Fe^{3+} from 0 to 1 in a solution of [Fe^{3+}] + [RBMAB] with a total concentration of 50 μmol L^{-1}. The Job's plot analysis revealed an approximate maximum at the 0.5 mole fraction, which indicates a 1:1 stoichiometry for the RBMAB-Fe^{3+} complex (Figure 4).

Fluorescence spectral response of RBMAB

To further understand the selectivity of RBMAB for Fe^{3+}, the changes in fluorescence intensity after various metal ions were

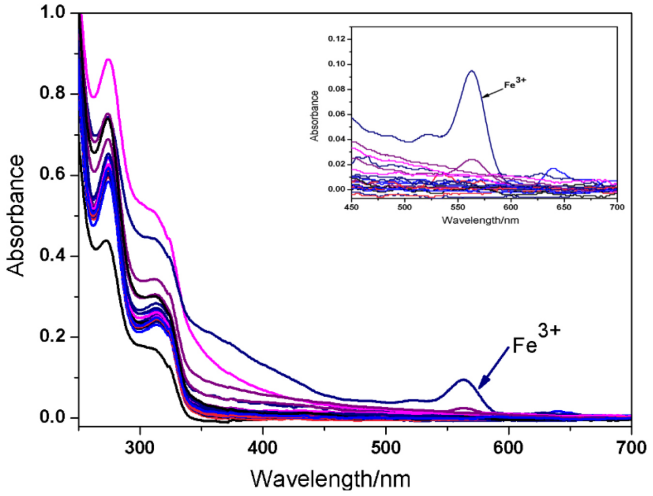

Figure 3. *UV-Vis absorbance spectra of RBMAB (20 μmol L^{-1}) in the absence and presence of 10 equivalents of various metal ions: Ag^{+}, Al^{3+}, Ba^{2+}, Ca^{2+}, Cd^{2+}, Co^{2+}, Cr^{3+}, Cs^{2+}, Cu^{+}, Cu^{2+}, Fe^{2+}, Fe^{3+}, Hg^{2+}, K^{+}, Li^{+}, Mg^{2+}, Mn^{2+}, Na^{+}, Ni^{2+}, Pb^{2+} and Zn^{2+}*

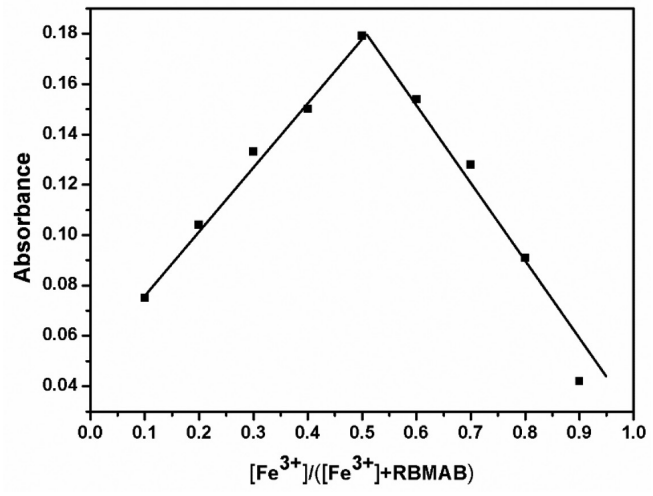

Figure 4. *Job's plot of RBMAB in an ethanol-H_2O (3:2, v/v, PBS buffer, 1.2 μmol L^{-1}, pH 7.2) solution with a total concentration of [RBMAB] +Fe^{3+} = 50 μmol L^{-1}. The absorption wavelength was 562 nm*

added under identical conditions were also investigated. The fluorescence spectra of RBMAB (20 μmol L^{-1}) in an ethanol-H_2O (3:2 v/v, PBS buffer, 1.2 mmol L^{-1}, pH 7.2) solution exhibits a notably weak fluorescence at 582 nm (λex = 562 nm) in the absence of metal ions, which indicates that the predominant form of RBMAB is the spirolactam form. When Fe^{3+} (200 μmol L^{-1}, 10 eq.) was introduced to the RBMAB solution, a remarkable fluorescence enhancement was observed (Figure 5), which indicates that the Fe^{3+} ions induce the formation of the strongly fluorescent, ring-opened RBMAB-Fe^{3+} complex (Scheme 2).The fluorescence enhancement of Fe^{3+} to RBMAB is as high as 180-fold. Other metal ions showed no obvious fluorescence enhancement under the same conditions. These results further demonstrate that RBMAB can function as a highly sensitive and selective fluorescent chemosensor for Fe^{3+} over various other metal ions.

The Fe^{3+} titration against RBMAB in an ethanol-H_2O (3:2 v/v, PBS buffer, 1.2 mmol L^{-1}, pH 7.2) solution was monitored using fluorescence spectra. As shown in Figure 6, when no Fe^{3+} ion was added to the RBMAB solutions, free RBMAB (20 μmol L^{-1}) remained colorless and exhibited notably weak fluorescence (λex = 562 nm) at

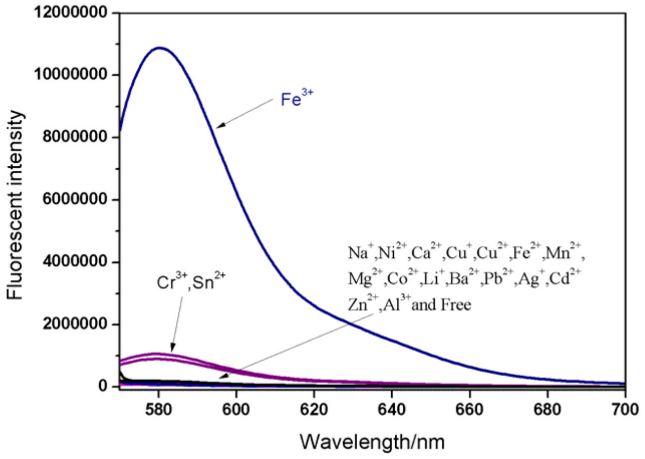

Figure 5. *Fluorescence spectra of RBMAB (10 μmol L^{-1}) in the absence and presence of 10 equivalents of various metal ions: Ag^{+}, Al^{3+}, Ba^{2+}, Ca^{2+}, Cd^{2+}, Co^{2+}, Cr^{3+}, Cs^{2+}, Cu^{+}, Cu^{2+}, Fe^{2+}, Fe^{3+}, Hg^{2+}, K^{+}, Li^{+}, Mg^{2+}, Mn^{2+}, Na^{+}, Ni^{2+}, Pb^{2+} and Zn^{2+}*

582 nm. However, when Fe^{3+} (0-400 μmol L^{-1}) was added, the titration of Fe^{3+} ions with RBMAB significantly increased the emission intensity at 582 nm, which resulted in a color change from colorless to pink, which can be ascribed to the formation of the ring-opened amide form of RBMAB upon Fe^{3+} ion binding (Scheme 2). The emission intensity reached its maximum value after the addition of 16 equivalents of Fe^{3+}. A fluorescence enhancement of over 800-fold was observed under saturation conditions. The competitive selectivity of RBMAB for Fe^{3+} in the presence of many other metal ions under identical conditions was also investigated. As shown in Figure 7 no significant variation in emission of the RBMAB- Fe^{3+} complex was observed compared with the results obtained with or without other metal ions. These results indicate that the detection of Fe^{3+} is not interfered by other metal ions and that RBMAB can be used as a selective Fe^{3+} fluorescent chemosensor.

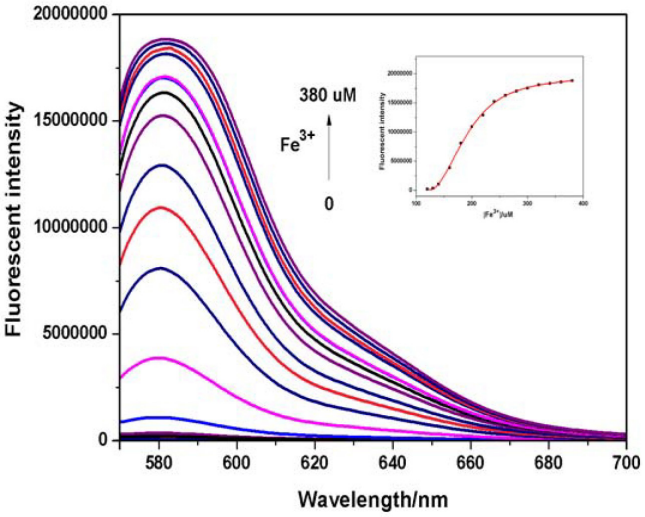

Figure 6. *Fluorescence spectra of RBMAB (20 μmol L^{-1}) when different amounts of Fe^{3+} were added.*

The association constant was calculated using the Benesi-Hildebrand plot: $F\text{-}F_0=[Fe^{3+}](F_{max}\text{-}F_0)/(1/K_a+[Fe^{3+}])$,[11] based on a 1:1 stoichiometry, where F is the obtained fluorescence intensity, F_0 is the fluorescence intensity of free RBMAB at the emission wavelength, and Fmax is the saturated fluorescence intensity of the RBMAB-Fe^{3+}

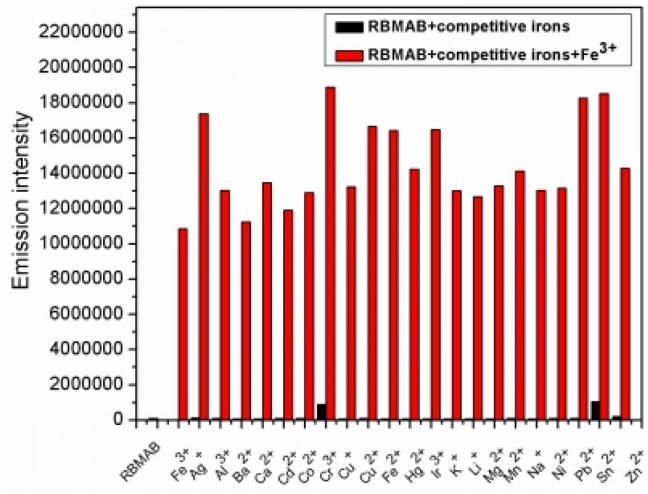

Figure 7. *Metal-ion selectivity profiles of RBMAB (10 μmol L^{-1}). The black bars represent the fluorescence intensity (582 nm) of RBMAB in the presence of 10 eq. of free ions in the absence of Fe^{3+} while the red bars represent after the addition of Fe^{3+}*

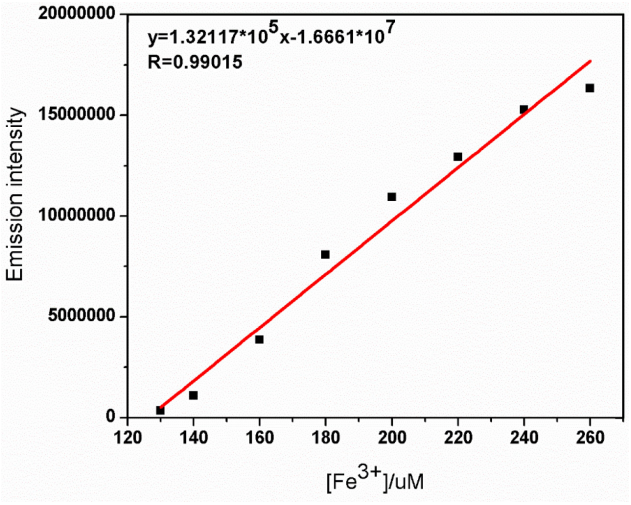

Figure 9. *Fluorescence intensity at 582 nm of RBMAB (20 μmol L^{-1}) in an ethanol-H_2O (3:2 v/v, PBS buffer, 1.2 mmol L^{-1}, pH 7.2) solution with different amounts of Fe^{3+}. The excitation wavelength is 562 nm*

complex. As shown in Figure 8, a linear relationship was obtained, and the binding constant was calculated to be 2.34×10^4 L $mmol^{-1}$ in an ethanol-H_2O (3:2 v/v, PBS buffer, 1.2 mmol L^{-1}, pH 7.2). The detection limit of RBMAB for Fe^{3+} was also calculated based on the fluorescence titration using the following equation: Detection limit = 3SD/*S,* where SD is the standard deviation of the blank and *S* is the slope of the calibration curve. The fluorescence emission spectrum of RBMAB was measured 10 times, and the standard deviation of the blank measurement was calculated. To obtain the slope, the ratio of fluorescence intensity at 582 nm was plotted versus the Fe^{3+}concentration (Figure 9). Thus, the calculated detection limit was 0.021 μmol L^{-1} (Supporting Material).

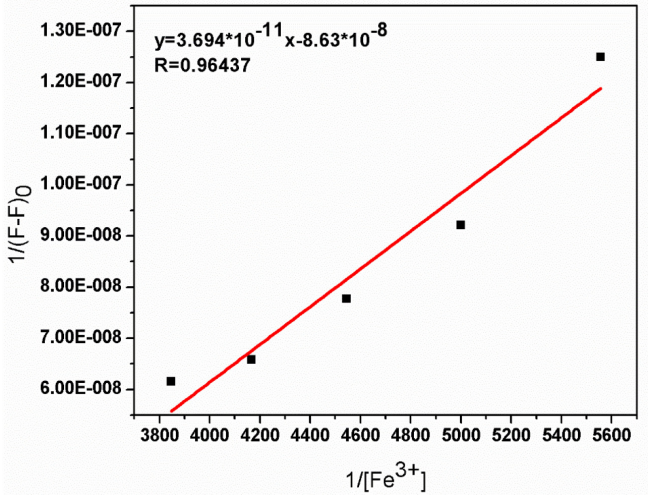

Figure 8. *Benesi-Hildebrand plot (λem= 582 nm) of 1/(F - F_0) vs. 1/[Fe^{3+}] based on a 1:1 association stoichiometry between RBMAB and Fe^{3+}*

^{1}H NMR study of RBMAB with Fe^{3+}

The ^{1}H NMR spectra of RBMAB in the presence and absence of Fe^{3+} were also investigated to further elucidate the nature of the interaction between Fe^{3+} and RBMAB. As shown in Figure 10, after 0.2 equivalent of Fe^{3+} was added to RBMAB in a CD_3OD:D_2O (5:1 v/v) solution, the proton signals of H_e, H_f and H_g displayed apparent downfield shifts from the peaks, which were centered at 6.421 ppm, 6.371 ppm and 6.327 ppm to two broad peaks, which were centered at 6.756 ppm and 6.569 ppm, respectively. These shifts originate from the Fe^{3+}-induced ring-opening process of the rhodamine B spirocycle. This indicates the coordination of RBMAB and Fe^{3+}, which was proposed in Scheme 3, where Fe^{3+} may be coordinated with one oxygen atom and two nitrogen atoms on the side chain of RBMAB.

Density functional theory (DFT) calculations

To better understand the nature of the coordination of Fe^{3+} with RBMAB, the energy-optimized structures of RBMAB and RBMAB-Fe^{3+} (Figure 11) were obtained using DFT calculations with the B3LYP method, where 6-31+G(d,p) was the basis set. The spatial distributions and orbial energies of the HOMO and LUMO of RBMAB and RBMAB-Fe^{3+} were also generated using DFT calculations (Figure 12). The results indicate that RBMAB, the HUMO was spread over the side benze moiety, whereas the HOMO was distributed on the spirolactam of rhodamine B moiety. The π electron on the HOMO of the RBMAB-Fe^{3+} complex were also mainly located on the side benze moiety, whereas the LUMO was mostly located on the guest Fe^{3+} ion. The energy gaps between the HOMO and LUMO in the probe RBMAB and RBMAB-Fe^{3+} were calculated to be 91.2 kcal mol^{-1} and 63.5 kcal mol^{-1} respectively. The results show that the binding of Fe^{3+} to RBMAB decreases the HOMO-LUMO energy gap of the complex and stabilizes the system.

Cell studies of RBMAB in the presence of Fe^{3+}

Because of its favorable molecular properties, RBMAB should be suitable for fluorescence imaging in living cells. Therefore, we further evaluated the applicability of RBMAB as a fluorescent probe for Fe^{3+} through *in vitro* cell studies. The direct detection of Fe^{3+} in living cells using the probe RBMAB was examined using cultured human cells (L-02). The cells were incubated with 0.1 mmol L^{-1} $FeCl_3$ in 50 mmol L^{-1} PBS buffer for 30 min at room temperature and subsequently incubated with the probe 20 μmol L^{-1}. RBMAB at 37 °C under 5% CO_2 for additional 120 min. Fluorescence microscopic studies show a lack of fluorescence for human L-02 cells after they were treated with only RBMAB (Figure 13e). After incubation with $FeCl_3$, a bright fluorescence was observed in L-02 cells (Figure 13f). The phase-contrast images in the bright fields of the cells show that the cells were viable during the experiments, which indicates that

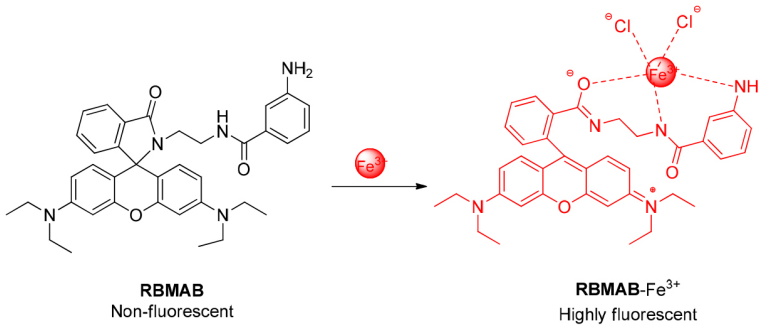

Scheme 3 *Proposed complexation mechanism of RBMAB with* Fe^{3+}

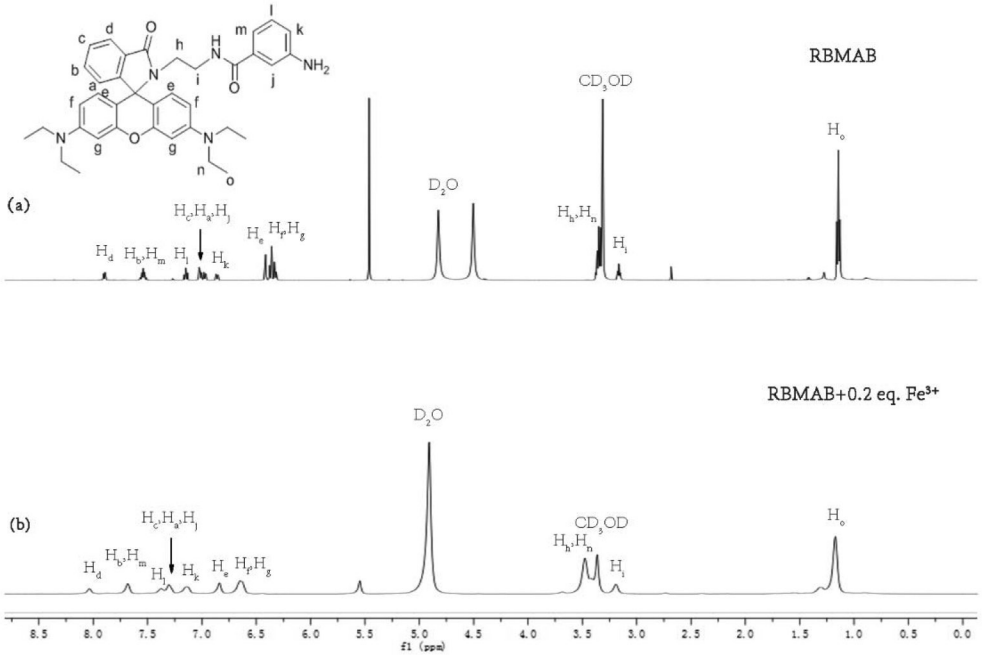

Figure 10. *^{1}H NMR spectra (500 MHz, 298K, methanol-d4:D_2O (5:1 v/v)) of (a)RBMAB and (b) RBMAB +0.2 equivalent* Fe^{3+}

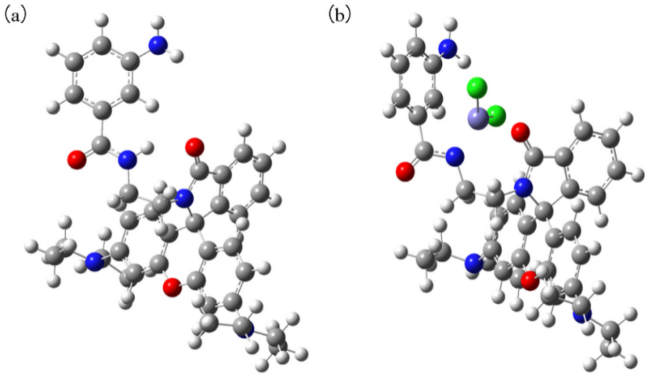

Figure11. Energy-minimized *structures of (a) RBMAB and (b) RBMAB-*Fe^{3+}

RBMAB may be cell-permeable and non-toxic to the cells.

To evaluate the cytotoxicity of RBMAB, the cell viability was determined using a

MTT assay in L-02 cells with RBMAB concentrations of 0-20 μmol L^{-1}. When RBMAB was incubated with L-02 cells for 48 h, it showed no toxicity to the cells (Figure 14). These results suggest that RBMAB may be suitable to be used as a potential probe to detect Fe^{3+} in biological samples.

CONCLUSIONS

In summary, a new rhodamine B derivative, RBMAB, was designed and synthesized as a highly selective chemosensor for Fe^{3+} ions in an ethanol/PBS (3:2 v/v; 1.2 mmol L^{-1}, pH 7.2) solution. The chemical structure of RBMAB was analyzed using ^{1}H NMR, ^{13}C NMR and HRMS. The 1:1 coordination mode was proposed based on a Job's plot. It has a low detection limit of 0.021μm . The Fe^{3+} binding ability of RBMAB was further demonstrated using DFT calculations, which suggest that the binding of RBMAB decreases the HOMO-LUMO energy gap of the complex. Cell studies further demonstrate that RBMAB can be a potential probe to detect Fe^{3+} in human liver cells (L-02).

SUPPLEMENTARY MATERIAL

The detailed characterization data for RBMAB, including ^{1}H NMR, ^{13}C NMR and HRMS can be found, in the online version, at http://www.quimicanova.sbq.org.br/ with free access.

ACKNOWLEDGMENTS

This work was supported by National Natural Science Foundation of China (21302098), the Fundamental Research Funds for the Central Universities (KJQN201415).

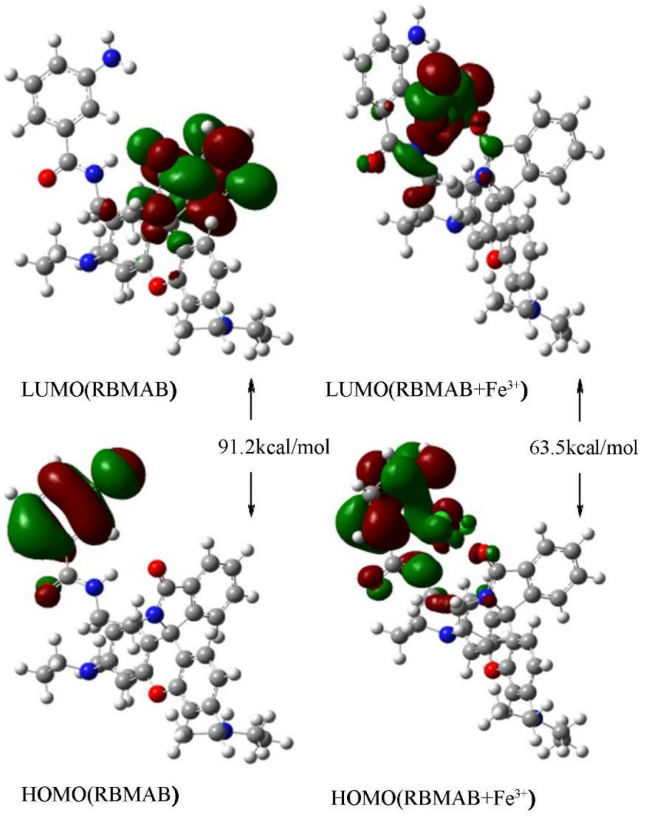

Figure 12. *HOMO and LUMO orbitals of (A) RBMAB and (B) the RBMAB-Fe^{3+}*

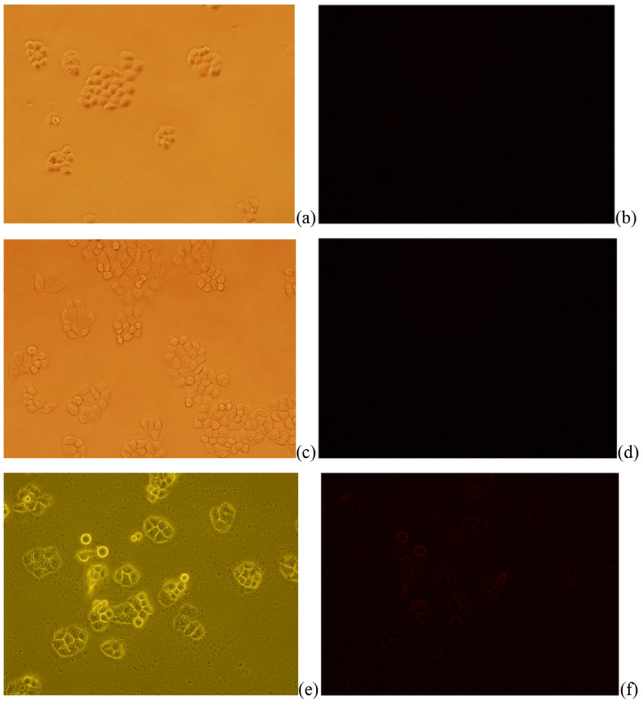

Figure 13 *Fluorescence images of human L-02 hepatocytes incubated with RBMAB and/or Fe^{3+}. The L-02 cells were incubated with 0.1 mmol L^{-1} $FeCl_3$ in 50 mmol L^{-1}PBS buffer for120 min at room temperature, followed by 20 μmol L^{-1} RBMAB for additional 30 min (**e**: bright-field image; **f**: fluorescence image). The DMSO-treated cells were taken as a control (**a**: bright-field image; **b**: fluorescence image), and only RBMAB-treated cells were also taken as a control (**c**: bright-field image; **d**: fluorescence image).*

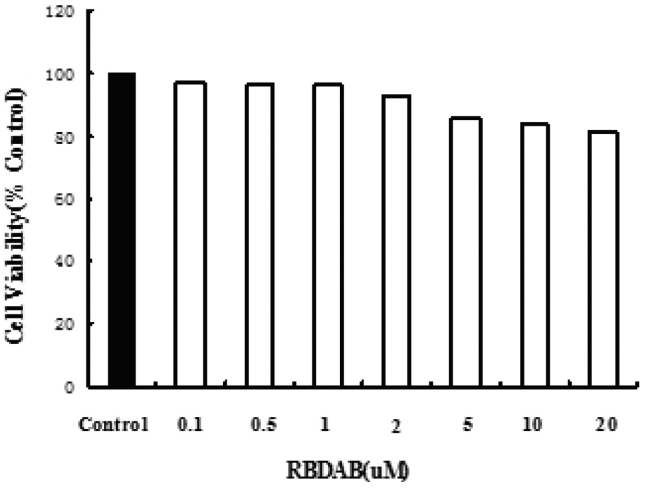

Figure 14. *Cytotoxicity of RBMAB in human L-02 hepatocytes. The cells were treated with different concentrations of RBMAB for 48 h, and the cell viability assay was determined using an MTT assay*

REFERENCES

1. Andrews, N. C.; *N. Engl. J. Med.* **1999**, *341*, 1986.
2. Steinmetz, H. T.; Tsamaloukas, A.; Schmitz, S.; Wiegand, J.; Rohrberg, R.; Eggert, J.; Thomas, L; *Supportive Care in Cancer* **2011**, *19*, 261.
3. Pietrangelo, A.; *N. Engl. J. Med.* **2004**, *350*, 2383.
4. Egan, T. J.; Hunter, R.; Kaschula, C. H.; *J. Med. Chem.* **2000**, *43*, 283.
5. Kienzl, E.; Puchinger, L.; Jellinger, K.; Linert, W.; Stachelberger, H.; Jameson, R. F.; *J. Neurol. Sci.* **1995**, *134*, 69.
6. Ong, W. Y.; Farooqui, A. A.; *J. Alzheimer's Dis.* **2005**, *8*, 183.
7. Ghaedi, M.; Shokrollahi, A.; Kianfar, A. H.; Mirsadeghi, A. S.; Pourfarokhi, A.; Soylak, M.; *J. Hazard Mater.* **2008**, *154*, 128.
8. Yaman, M.; Kaya. G.; *Anal. Chim. Acta* **2005**, *540*, 77.
9. Scheers, N.; Andlid, T.; Alminger, M.; Sandberg, A. S.; *Electroanalysis* **2010**, *22*, 1090.
10. Sahoo, S. K.; Sharma, D.; Bera, R. K.; Crisponi, G.; Callan, J. F.; *Chem. Soc. Rev.* **2012**, *41*, 7195.
11. Yang, Y.; Gao, C. Y.; Zhang, N.; Dong, D.; *Sens. Actuators, B* **2016**, *222*, 741.
12. Wilson, A. D.; *Analyst* **1960**, *85*, 823.
13. Patil, N. B.; Bhide, S. V.; Kale, N. R.; *Carbohydr. Res.* **1973**, *29*, 513.
14. Kwon, J. Y.; Jang, Y. J.; Lee, Y. J.; Kim, K. M.; Seo, M. S.; Nam, W.; Yoon, J.; *J. Am. Chem. Soc.* **2005**, *127*, 10107.
15. Ko, S. K.; Yang, Y. K.; Tae, J.; Shin, I.; *J. Am. Chem. Soc.* **2006**, *128*, 14150.
16. Tang, M.; Wen, G.; Luo, Y.; Kang, C.; Liang, A.; Jiang, Z.; *Luminescence* **2015**, *30*, 296.
17. Gao, T.; Lee, K. M.; Yang, S. I.; *J. Toxicol. Environ. Health Sci.* **2009**, *1*, 159.
18. Ju, H.; Lee, M. H.; Kim, J.; Kim, J. S.; Kim, J.; *Talanta*, **2011**, *83*, 1359.
19. Zhou, Y.; Wang, F.; Kim, Y.; Kim, S. J.; Yoon, J.; *Org. Lett.* **2009**, *11*, 4442.
20. Zhang, J. F.; Zhou, Y.; Yoon, J.; Kim, Y.; Kim, S. J.; Kim, J. S. ; *Org. Lett.* **2010**, *12*, 3852.
21. Yuan, Y.; Sun, S.; Liu, S.; Song, X.; Peng, X.; *J. Mater. Chem. B* **2015**, *3*, 5261.
22. Liu, W.; Xu, L.; Sheng, R.; Wang, P.; Li, H.; Wu, S.; *Org. Lett.* **2007**, *9*, 3829.
23. Shim, S.; Tae, J.; *Bull. Korean Chem. Soc.* **2011**, *32*, 2928.
24. Wan, Y.; Guo, Q.; Wang, X.; Xia, A.; *Anal. Chim. Acta* **2010**, *665*, 215.
25. Li, M.; Zhang, D.; Liu, Y.; Ding, P.; Ye, Y.; Zhao, Y.; *J. Fluoresc.* **2014**, *24*, 119.

26. Huang, J.; Xu, Y.; Qian, X.; *J. Org. Chem.* **2009**, *74*, 2167.
27. Wu, J. S.; Hwang, I. C.; Kim, K. S.; Kim, J. S.; *Org. Lett.* **2007**, *9*, 907.
28. Chereddy, N. R.; Thennarasu, S.; Mandal, A. B.; *Analyst* **2013**, *138*, 1334.
29. Weerasinghe, A. J.; Schmiesing, C.; Varaganti, S.; Ramakrishna, G.; Sinn, E.; *J. Phys. Chem. B* **2010**, *114*, 9413.
30. Aydin, Z.; Wei, Y.; Guo, M.; *Inorg. Chem. Commun.* **2012**, *20*, 93.
31. Zhang, L.; Fan, J.; Peng, X.; *Spectrochim. Acta, Part A* **2009**, *73*, 398.
32. Tang, L.; Li, Y.; Nandhakumar, R.; Qian, J.; *Monatsh. Chem.* **2010**, *141*, 615.
33. OuYang, H.; Gao, Y.; Yuan, Y.; *Tetrahedron Lett.* **2013**, *54*, 2964.
34. Liu, Y.; Xu, Z.; Wang, J.; Zhang, D.; Ye, Y.; Zhao, Y.; *Luminescence* **2014**, *29*, 945.
35. Li, G.; Tang, J.; Ding, P.; Ye, Y.; *J. Fluoresc.* **2016**, *26*, 155.
36. Bao, X.; Shi, J.; Nie, X.; Zhou, B.; Wang, X.; Zhang, L.; Pang, T.; *Bioorg. Med. Chem.* **2014**, *22*, 4826.